Islanding of a Topologically Realistic Rural Grid Using Grid-Forming Inverters

Vinson Guov
School of EECS
Oregon State University
Corvallis, OR, U.S.A.
guovv@oregonstate.edu

Yue Cao
School of EECS
Oregon State University
Corvallis, OR, U.S.A.
Yue.Cao@oregonstate.edu

Ian Beil
Grid Edge Solutions
Portland General Electric
Portland, OR, U.S.A.
Ian.Beil@pgn.com

***Abstract*—As future electric grids become increasingly renewable dependent, microgrids will become a powerful mechanism in maintaining or improving grid resiliency. This paper studies the emergency islanding of a rural grid using grid-forming inverter-based resources. A grid-forming inverter model is developed with a hierarchical control approach, and a synthetic grid model is produced to emulate the topology of a rural system in northwest Oregon, based on input from the local utility. A simulation of central versus distributed placement of inverters within the rural microgrid is performed to study the dynamics during events such as grid disconnection and loss of a transmission line, and to observe the power-sharing between multiple inverters.**

***Index Terms*—Grid-forming Inverter, Distributed Generation, Rural Grid, Microgrid, Grid Resilience, Islanding, Natural Disasters, Wildfires, Solar PV**

I. Introduction

As the presence of renewable energy sources (RES) on the grid continues to accelerate, a significant share of that growth is felt by rural power systems. Naturally, many rural areas are optimal locations for RESs due to the availability of renewables, such as photovoltaic solar farms and wind turbines. However, integrating many DERs into a rural grid is challenging because they are generally weak grids with low short-circuit ratio (SCR) and low X/R ratio. Rural grids are typically supplied by few transmission lines, resulting in poor voltage regulation.

This paper focuses on a rural grid threatened by a high risk of wildfires [1]. The excessive smoke and particulate matter produced by wildfire may cause transmission lines to arc and trip intermittently. This forces utilities to take the lines offline until conditions improve to preserve the stability of the larger power system [2]. Additionally, if transmission lines continue to operate during high fire danger conditions, this may cause wildfires if the line arcs to nearby vegetation and trees [3]. Without available generation supplied by operational lines, downstream customers will experience a loss of electricity supply.

Grid-forming inverter-based resources (IBR) present an opportunity to reduce downtime during such emergencies by enabling intentional islanding of rural areas. The rural island will contain distributed generation alongside the loads to be self-sustaining [4]. Photovoltaic solar and battery energy storage systems (BESS) could be deployed in tandem at several locations on this island to provide power at several buses. Since there are no available synchronous generators connected to this island, a grid-forming inverter must establish a reference frequency [5]. In Greece in 2007, mobile diesel generators were reactively deployed to supply ad hoc low-voltage microgrids using the existing distribution network [6]. This solution may be applied proactively to high wildfire risk areas by performing studies to determine the optimal placement of grid-forming resources and accompanying BESS.

The case study performed examines the behavior of the inverters during transient events and their impact to the power quality and stability of the intentional island. The first part of this paper focuses on developing a grid-forming inverter model based on [7]. This model will be used within a developed rural power system model to investigate grid-forming IBRs placed in a *centralized or distributed* arrangement to supply the rural microgrid during emergency islanding. The second part of this paper will describe the characteristics of the rural grid. Instead of using a generalized test grid, this study develops a synthetic transmission system model informed by the topology of the rural network located near Mount Hood, Oregon, USA. While the actual voltage levels, system impedance, etc. have been adjusted, the arrangement of the near-radial transmission system is preserved. Using a realistic grid will demonstrate the unique challenges utilities face as they improve grid resilience while distributed generation continues to grow. This type of study applies to the planning and preparation of intentional islands, which varies depending on reliability/resiliency goals and the topological risks of the grid being studied. This paper will conclude with simulation results, primarily focusing on the dynamics experienced by the island in either centralized or distributed IBR placement strategies. This will include the transients which occur when switching between grid-connected and island operation, and during contingencies such as loss of a line or loss of an inverter.

II. Grid Forming Inverter Model

Since a detailed discussion of the grid-forming inverter is not the main focus of this paper, readers are referred to [7] and [8] for more information on the control systems used in this paper. The grid-forming inverter model is developed in EMTP simulation software and consists of three hierarchical levels of control based on [7]. EMTP was chosen because of its ability to accurately model transient behavior in a large power system.

A. Primary control

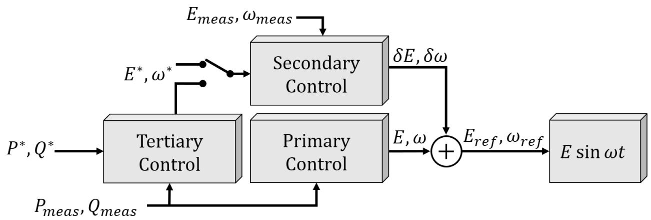

Fig. 1. Inverter hierarchical control block diagram

The inverter mimics the primary control behavior of a synchronous generator by implementing droop control, enabling power sharing and frequency synchronization. This primary control loop regulates voltage and frequency output depending on real and reactive power output, using droop functions (1) and (2) from [7], where $G_P(s)$ and $G_Q(s)$ are coefficients that control the maximum Δw and ΔE depending on available inverter power [7]. In this paper, $G_P(s)$ and $G_Q(s)$ are constants because the inverters are assumed to be unconstrained in power output. In reality, the power output will be constrained by the energy source and storage, which may fluctuate temporally if the source is renewable, such as solar PV.

$$\omega = \omega' - G_P(s) * (P_{meas} - P') \tag{1}$$

$$E = E' - G_Q(s) * (Q_{meas} - Q') \tag{2}$$

B. Secondary control

When an inverter experiences a sudden change in load, frequency and voltage may not return to nominal values without additional control effort. This control loop provides restoration to the nominal voltage/frequency setpoints using PI controllers described by (3) and (4). Before connecting the inverter to a grid, synchronization is required to ensure little to no power exchange between the grid and microgrid when the connection switch closes. A PLL is used to produce the $\Delta\omega_{sync}$ to achieve synchronization [7]. $\Delta\omega_{sync}$ is zero when grid synchronization is off. The PLL is not used when grid synchronization is not needed.

$$\delta E = k_{pE}(E^* - E_{meas}) + k_{iE} \int (E^* - E_{meas})dt \tag{3}$$

$$\delta\omega = k_{pw}(\omega^* - \omega_{meas}) + k_{iw} \int (\omega^* - \omega_{meas})dt + \Delta\omega_{sync} \tag{4}$$

C. Tertiary control

Tertiary control regulates the import and export of power from the microgrid to the grid when the microgrid is operating in grid-connected mode. This paper uses tertiary control to manage the power flow from each inverter instead of the entire microgrid. Setpoints are given to the controller, and two PI controllers based on (5) and (6) adjust the voltage and frequency of the inverter to regulate real power and reactive power flowing to and from the grid [7].

$$\omega^* = k_{pP}(P^* - P_{meas}) + k_{iP} \int (P^* - P_{meas})dt \tag{5}$$

$$E^* = k_{pQ}(Q^* - Q_{meas}) + k_{iQ} \int (P^* - P_{meas})dt \tag{6}$$

D. Hierarchical control structure

Fig. 1 shows the relationships between the control levels. Primary control is always active and is responsible for V/f and Q/V droop. Secondary control provides additional control effort which is summed with the droop control output to correct the voltage and frequency steady-state error. Secondary control responds slower than primary control and regulates voltage and frequency output over a larger time frame. Additionally, if power output control is desired, tertiary control will feed a dynamic E^* and ω^* to secondary control to achieve real and reactive power output targets. The controller then outputs a reference sinusoid to generate the three-phase voltage waveforms.

E. Power electronics

Power electronics hardware design is not the focus of this study and would reduce the generality of this inverter model. Power electronic specifications are unknown, so an average model is used. The inclusion of power electronics switching modeling would also lengthen the simulation times in EMTP, requiring a smaller time-step size to capture switching dynamics.

III. Rural Grid Model

The synthesized transmission system model is informed by the topology of the rural network located near Mount Hood, Oregon, USA. This rural area is heavily forested and presents a wildfire risk. In order to preserve confidential data, the specific grid topology has been adjusted, as have all system voltages (for instance, the actual system is 57 kV, not 69 kV). The rural grid receives most of its electricity supply from an adjacent urban center through a few transmission lines. The rural network supplies power to the area in a radial fashion, primarily through overhead 69 kV transmission lines spanning about 40 miles. At the end of this radial network, a long 34.5 kV underground cable transmits power to a remote area, which is the only transmission line/cable not at risk of experiencing an wildfire-induced arc fault. A transformer is used to step 69 kV down to 34.5 kV for the underground cable. Another transformer steps down 34.5 kV to 13.8 kV to supply Bus 10.

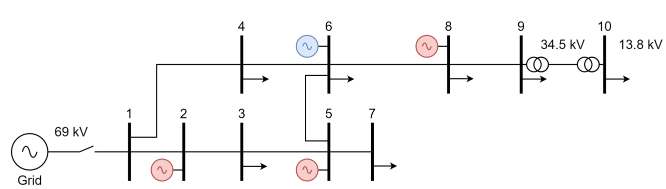

Fig. 2. Rural grid one-line diagram with centralized (blue) and distributed inverters (red)

TABLE I
LOAD PARAMETERS

Bus	Real Power (MW)	Reactive Power (MVAR)
3	20.7	4.5
4	13.7	5.0
6	6.7	1.4
7	26.7	3.8
8	4.2	1.0
9	6.5	0.7
10	3.0	0.9

TABLE II
TRANSMISSION LINE PARAMETERS

Line		Parameters			
From Bus	To Bus	Ω/mi	mH/mi	μF/mi	Length (mi)
1	2	0.1771	2.398	0.0130	1.5
1	4	0.1734	2.349	0.0128	5.4
2	3	0.1737	1.378	0.0223	3.7
3	5	0.1715	2.378	0.0126	4.7
4	6	0.1740	2.298	0.0131	4.5
5	6	0.1718	2.382	0.0127	0.8
5	7	0.4088	2.416	0.0124	2.8
6	8	0.2726	2.386	0.0126	15.0
8	9	0.2495	2.419	0.0126	5.0
9	10	0.7251	1.462	0.1310	12.9

As seen in Fig. 2, the two largest loads in this rural grid exist on the radial leg which spans from Bus 1 to Bus 7, to a total of 47.4 MW and 8.3 MVAR. The other radial leg is longer and spans from Bus 4 to Bus 10, with loads totaling to 34.1 MW and 9 MVAR. The loads, listed in Table I, are power constant in this study and represent typical loads based on historic data. There is a three-terminal junction at Bus 5, connecting the two radial legs together to allow power flow between Buses 5 and 6. For this study, Bus 1 is assumed to be connected to a stiff grid source. This assumption is valid since the bulk grid has substantial inertia. In the future when renewable penetration is high, this may not be a valid assumption anymore, requiring extensive modeling. The switch in Fig. 2 between the grid source and Bus 1 represents the point of common coupling (PCC) between the bulk grid and the rural microgrid, and allows the rural grid to island.

The transmission lines are modeled in EMTP using the constant parameter line model, which is mathematically equivalent to an infinite series of PI lines [10]. This line model has a time-step constraint, which is required to accurately model the propagation delay of the traveling waves. The exceptions are lines 1-2 and 5-6. Those two lines were accurately modeled as single PI-lines because they are short enough to neglect traveling waves, which allows the simulation to run a larger minimum simulation time-step size. The transmission line per-length parameters are listed in Table II.

IV. SIMULATION STUDY

A case study performed in EMTP combines the inverter model described in Section II and rural grid data from Section III to simulate the dynamics of the rural grid when it is temporarily islanded and solely sustained by deployed renewable grid-forming inverter resources with energy storage, such as during a wildfire when the risk of frequent line faults is high and lines are intentionally opened to reduce stability risks. The study covers the transition from grid-connected to microgrid mode and the transient response to a line tripping open and a loss of an inverter.

A. Centralized vs. Distributed Inverters

The case study discussed in this paper is a proactive inquiry into whether emergency islanding is realizable, so it is relevant to compare different IBR placement strategies. On one hand, it is easier for a utility to place emergency IBRs at a centralized location. On the other hand, distributed IBRs at different buses will place available generation closer to all loads within the island, improving power quality at the cost of deployment time and resources. In the centralized generation scenario, an IBR is placed at Bus 6, represented by a blue-colored source in Fig. 2. In the distributed generation scenario, IBRs are placed at Buses 2, 5, and 8, represented by the red-colored sources in Fig. 2. Since the total load of this island is large, this may physically consist of multiple parallel IBRs working in tandem at a bus, but this paper will model inverters at each bus as a single large inverter. The distributed inverters are expected to power-share such that each distributed inverter will deliver roughly a third of the power of the centralized inverter. These two separate scenarios will be simulated and their performance characteristics compared.

B. Simulation

The EMTP simulations used a time-step of 15μs. Ultimately, the minimum propagation delay of the transmission lines determines the maximum simulation time-step size. The propagation delay of the transmission lines is mostly affected by line length.

In both simulations, the rural grid starts in grid-connected mode with no IBRs connected. At t = 0 s, the inverters enable grid synchronization via PLL to match its voltage output phase to their respective PCCs' voltage phase, while disconnected from the grid. For the *centralized* inverter, at t = 1 s, the inverter connects to the grid and enables tertiary control to ramp its generation to match the island's load. For the *distributed* inverters, the same event occurs but in a staggered fashion to demonstrate tertiary power control, with inverters at Buses 8, 2, and 5 connecting at t = 0.8 s, t = 0.9 s, and t = 1 s, respectively. The power flow from the stiff grid into the rural grid is driven to zero just before t = 3 s, preparing the system for disconnection from the grid. For both scenarios, at t = 3 s, the stiff grid source is disconnected from Bus 1, entering the rural grid into islanded mode. After t = 3 s, all loads are satisfied by the microgrid's IBRs, and the inverters disable tertiary control and allow secondary control to regulate voltage and frequency at their respective buses.

To simulate a loss of a transmission line, the line between Buses 6 and 8 (the longest line in the rural grid) is taken offline at t = 6 s. This will cause of a loss of load in the centralized scenario, since there will no longer be generation available to Buses 8, 9 and 10 (and experience blackouts at those buses). In the distributed scenario, since there is an

IBR placed at Bus 8, it is expected to remain connected to the downstream buses/loads, so the island will be further split into two islands. This will demonstrate the grid-forming inverters' ability to continue power delivery after a topological disruption. The following list summarizes the events occurring during the simulations:

1) t = 0 s: Inverters disconnected, grid synchronization enabled
2) t = 1 s: Inverters connect, tertiary power control enabled to reduce grid power import to zero
3) t = 3 s: Grid disconnected from island
4) t = 6 s: Loss of line between Bus 6 and Bus 8

One of the advantages of having multiple generation sites is redundancy. If for any reason the inverters fail at a bus, two out of three generation sites can remain active and be able to compensate for the loss of generation. The loss of an inverter is simulated to test this capability, assuming each inverter has sufficient power.

The steady-state voltage profile of both radial legs of the island will be examined to understand the effect of installing grid-forming inverters within this island, in contrast to grid-connected mode where available generation is further away and supplied from outside of the rural grid.

C. Simulation Results

1) Centralized vs. Distributed Inverters: The simulation results comparing the two scenarios are shown in Fig 5 and 6. For these plots, the shaded colors correspond to the various time frames described in Section IV-B. The impact on Bus 10 due to the transient events are shown in Fig. 5d and 6d. For the central case, the voltage at Bus 10 becomes zero after the loss of a critical line. In distributed case, the loss of the same line does not result in a blackout at Bus 10, since a nearby inverter remains connected. The voltages at Bus 10 are also higher in the distributed scenario due to the closer proximity of an inverter.

To examine the transition from grid-connected to islanded operation, Fig. 5a and 6a show the power imported from the grid. The step changes in power in Fig. 6a indicate balanced power-sharing between the three inverters while tertiary control is active. The power output of each distributed inverter can be seen in Fig. 6b and 6c as each inverter comes online from t = 0.8 s to t = 1 s. Inverter 1 at Bus 8 experiences a drop in load due to its disconnection from the island at t = 6 s. However, all of the inverters are able to compensate for change in loads by adjusting their power outputs to maintain voltage.

2) Steady-state Voltage Profile: In the base case where no inverters are connected and the rural grid is supplied normally by the bulk grid, shown in Fig. 3, the voltage naturally drops as the distance increases from Bus 1, where the AC source is connected. The rise in voltage from Bus 9 to 10 can be seen at 30 to 43 miles away from Bus 1. This can be explained by the winding ratio of the two transformers connecting Bus 9 to 10, helping to reduce the voltage drop experienced at Bus 10, which is the furthest bus from available generation.

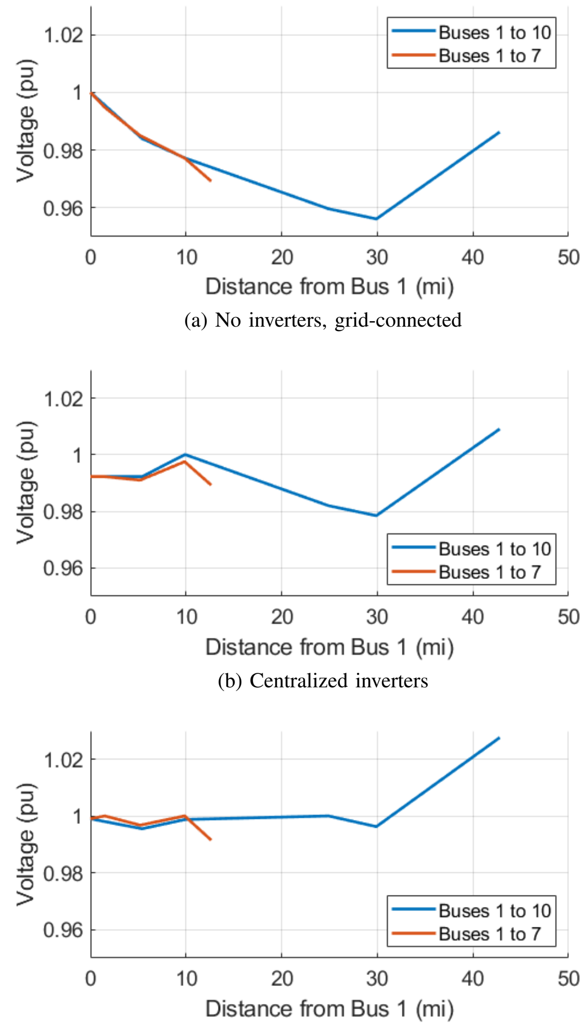

(a) No inverters, grid-connected

(b) Centralized inverters

(c) Distributed inverters

Fig. 3. Voltage profile of rural grid from different scenarios

There is a significant improvement in the voltage profile seen in either the centralized or distributed inverter scenario, with the distributed one exhibiting the best voltage regulation out of the three cases shown.

3) Loss of an Inverter: Starting from steady-state islanded operation in the distributed inverter scenario, Fig. 4 shows the power outputs of the inverters as one of the inverters, at Bus 5, is abruptly disconnected from the island. The impact this has on bus voltages is plotted in Fig. 4c. At t = 10 s, the inverter is disconnected, indicated by the step change to zero in real and reactive power output. The buses experience a brief brownout before recovering back to near nominal voltage, indicating a successful recovery.

4) Discussion: This study highlights the potential benefits of installing distributed generation in rural areas, improving voltage regulation with a fast response situated closer to the loads. This study demonstrates that for highly radial power system with little to no meshing, a distributed generation approach is more effective in preparing for line contingencies. However, the downside is that it would be more expensive to

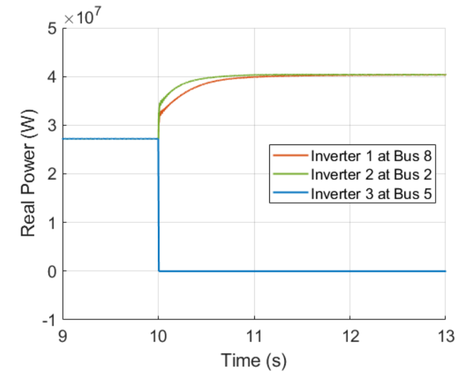

(a) Inverter real power output

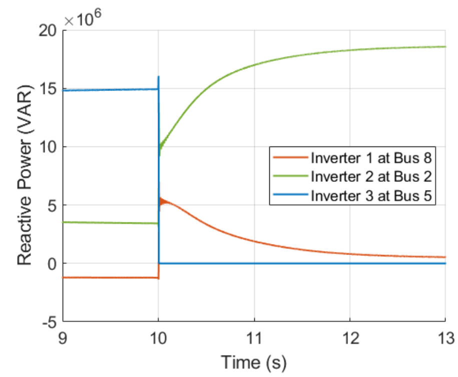

(b) Inverter reactive power output

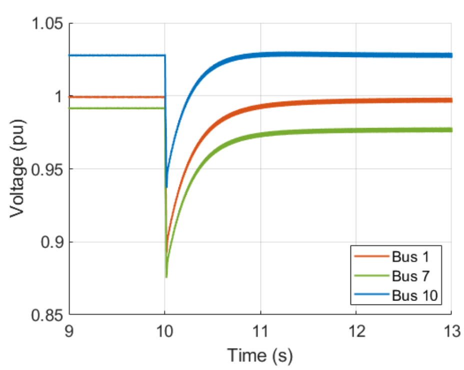

(c) Bus voltages

Fig. 4. Loss of one of three distributed inverters

deploy multiple inverter units at different sites during a natural disaster. If a natural disaster renders a certain area of the rural grid inaccessible, the centralized inverter arrangement may be better suited, and still manages to improve the bus voltage profile significantly compared to the base case. This case study did not consider the implications of this system lacking any real inertia, but literature suggests synthetic inertia will be an integral component of grid-forming inverter control.

V. Conclusion

This paper describes a case study in which two different IBR placement strategies are simulated in EMTP to perform emergency islanding of a rural grid during a natural disaster such as a wildfire. A hierarchical grid-forming inverter control approach and averaged power electronic inverter modeling are explained in Section II. In Section III, the characteristics of the rural grid are examined and modeled in EMTP using constant distributed parameter transmission line modeling. Section IV describes the simulation setup in EMTP and the grid events performed during the simulation, as well as the accompanying results and discussion. Both strategies successfully maintained voltage stability during transient events and changes in inverter control modes, with the distributed inverters demonstrating tertiary power control and shared power responsibility due to droop control laws. A loss of one of three inverters in the distributed scenario is also simulated, and demonstrates the ability of the remaining inverters to pick up the lost generation, preventing a blackout, assuming the inverters have sufficient power capability. The distributed scenario provides better stability to bus voltages on the poorly meshed rural grid during transient events but will require more resources to deploy during an emergency.

VI. Acknowledgement

This work was supported in part by Portland General Electric, Oregon, USA.

References

[1] R. Moreno et al., "From Reliability to Resilience: Planning the Grid Against the Extremes," *IEEE Power and Energy Magazine*, vol. 18, no. 4, pp. 41-53, July-Aug. 2020.

[2] T. Sickinger, *Oregon wildfire robs California of critical electricity supply from Pacific Northwest during heat wave*, Oregon Live, July 11, 2021. Accessed on January 31, 2021. [Online]. Available: https://www.oregonlive.com/wildfires/2021/07/oregon-wildfire-robs-california-of-critical-electricity-supply-from-pacific-northwest-during-heatwave.html

[3] H. Nazaripouya, "Power Grid Resilience under Wildfire: A Review on Challenges and Solutions," *IEEE Power & Energy Society General Meeting (PESGM)*, 2020, pp. 1-5.

[4] I. J. Balaguer, Q. Lei, S. Yang, U. Supatti and F. Z. Peng, "Control for Grid-Connected and Intentional Islanding Operations of Distributed Power Generation," *IEEE Transactions on Industrial Electronics*, vol. 58, no. 1, pp. 147-157, Jan. 2011.

[5] D. Pattabiraman, R. H. Lasseter. and T. M. Jahns, "Comparison of Grid Following and Grid Forming Control for a High Inverter Penetration Power System," *IEEE Power & Energy Society General Meeting (PESGM)*, 2018, pp. 1-5.

[6] R. Moreno et al., "Microgrids Against Wildfires: Distributed Energy Resources Enhance System Resilience," *IEEE Power and Energy Magazine*, vol. 20, no. 1, pp. 78-89, Jan.-Feb. 2022.

[7] J. M. Guerrero, J. C. Vasquez, J. Matas, L. G. de Vicuna and M. Castilla, "Hierarchical Control of Droop-Controlled AC and DC Microgrids—A General Approach Toward Standardization," *IEEE Transactions on Industrial Electronics*, vol. 58, no. 1, pp. 158-172, Jan. 2011.

[8] K. De Brabandere, B. Bolsens, J. Van den Keybus, A. Woyte, J. Driesen and R. Belmans, "A Voltage and Frequency Droop Control Method for Parallel Inverters," *IEEE Transactions on Power Electronics*, vol. 22, no. 4, pp. 1107-1115, July 2007.

[9] Q. Zhong and G. Weiss, "Static synchronous generators for distributed generation and renewable energy," *in Proc. IEEE/PES Power Systems Conference and Exposition*, 2009, pp. 1-6.

[10] H. W. Dommel, "Digital Computer Solution of Electromagnetic Transients in Single-and Multiphase Networks," *IEEE Transactions on Power Apparatus and Systems*, vol. PAS-88, no. 4, pp. 388-399, April 1969.

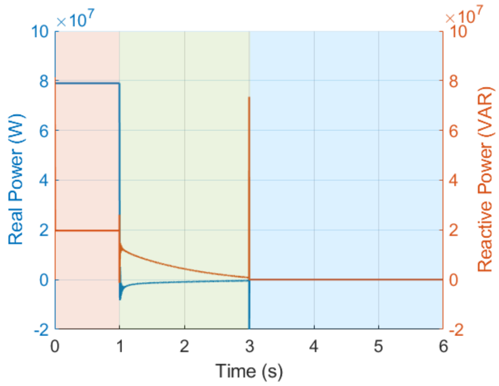

(a) Power imported from grid

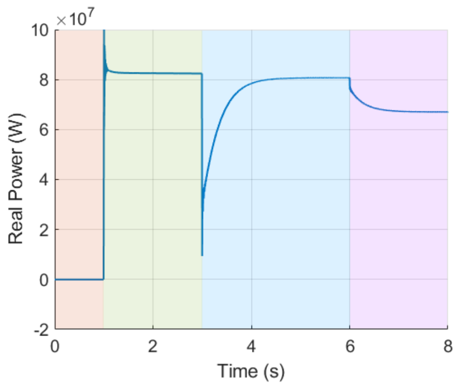

(b) Inverter real power output

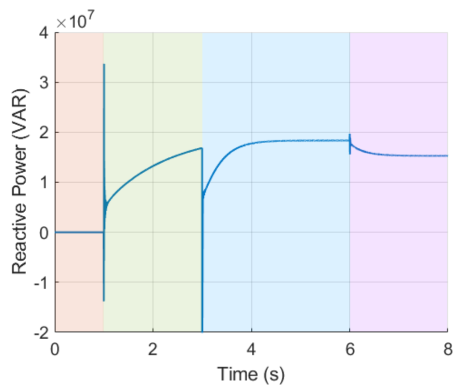

(c) Inverter reactive power output

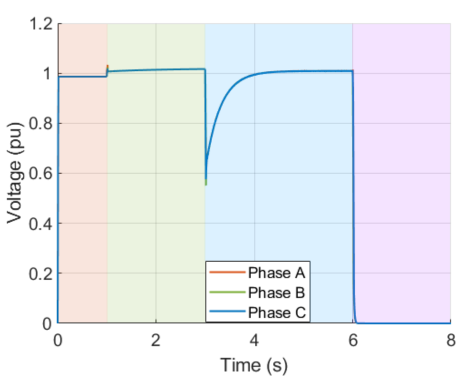

(d) Voltages at Bus 10

Fig. 5. Centralized inverters, grid disconnection and loss of line

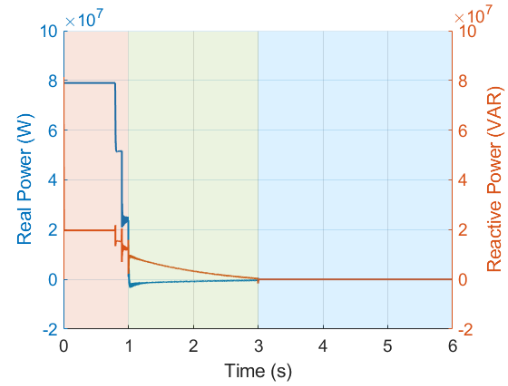

(a) Power imported from grid

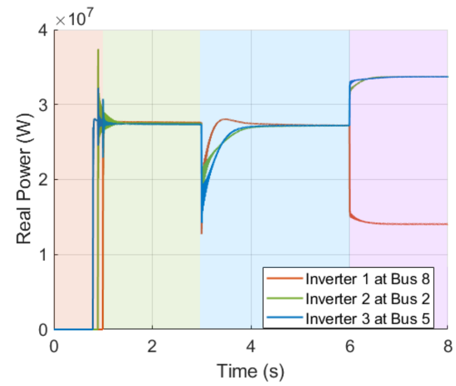

(b) Inverter real power output

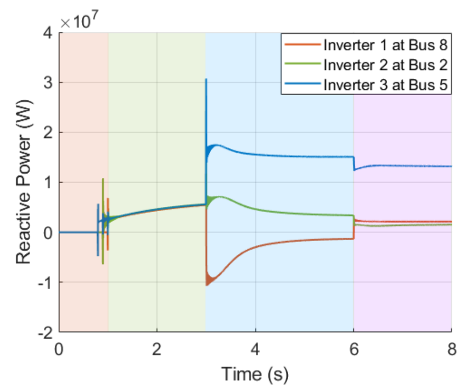

(c) Inverter reactive power output

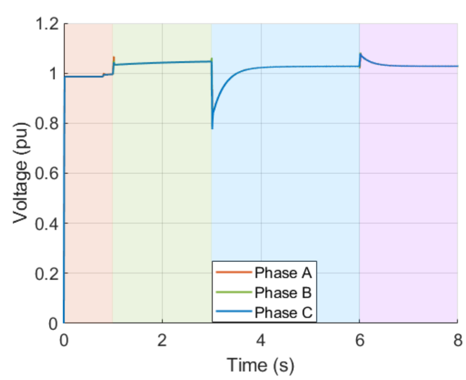

(d) Voltages at Bus 10

Fig. 6. Distributed inverters, grid disconnection and loss of line